NASA TECHNICAL MEMORANDUM

NASA TM X-68259

NASA TM X-68259

VELOCITY DECAY AND ACOUSTIC CHARACTERISTICS OF VARIOUS NOZZLE GEOMETRIES WITH FORWARD VELOCITY

by U. von Glahn, D. Groesbeck, and J. Goodykoontz
Lewis Research Center
Cleveland, Ohio 44135

TECHNICAL PAPER proposed for presentation at
Sixth Fluid and Plasma Dynamics Conference sponsored by
the American Institute of Aeronautics and Astronautics
Palm Springs, California, July 16-18, 1973

VELOCITY DECAY AND ACOUSTIC CHARACTERISTICS OF VARIOUS NOZZLE GEOMETRIES WITH FORWARD VELOCITY

by U. von Glahn, * D. Groesbeck, ** and J. Goodykoontz**

Lewis Research Center

ABSTRACT

Utilizing a static test stand, 6- by 9-foot wind tunnel and 13-inch circular free jet, aerodynamic and acoustic data were obtained with a convergent circular nozzle, bypass nozzle, 6-tube mixer nozzle, and 6-tube mixer nozzle with an ejector. The aerodynamic data consist of velocity decay surveys with and without forward velocity. The acoustic data include total sound power, directivity and frequency spectra obtained statically and with forward velocity. The relation of aerodynamic and acoustic measurements statically and in forward flight for the various nozzle configurations are discussed.

E-7547

INTRODUCTION

Propulsion system noise measurements usually are made in static ambient environmental surroundings. In order to predict inflight propulsion system noise (specifically jet exhaust noise), the interaction of the forward velocity of the aircraft with the jet exhaust velocity must be established. The ability to predict such interaction noise is important in the determination of the approach and takeoff flight path for minimum aircraft noise over a community.

A number of studies have been made in the last two decades in which noise measurements were made of aircraft flying by and compared with static ground tests (ref. 1). The results of these tests have indicated that forward velocity attenuates jet exhaust noise; however, the absolute attenuation magitudes have been varied and inconclusive. In an analytical

---

*Chief, Jet Acoustics Branch, member AIAA.

**Aerospace engineer.

Page Intentionally Left Blank

study (ref. 2), Ffowcs Williams suggested a subsonic jet noise reduction with forward velocity on the basis of the relative velocity (jet velocity minus forward velocity) to the seventh power multiplied by the jet velocity.

The present study, conducted at the NASA Lewis Research Center, considers the effect of forward velocity on the jet velocity decay characteristics and the associated acoustic characteristics. It was predicated in conducting these tests, that differing nozzle geometries with their associated velocity decay patterns would cause the forward velocity effect on jet noise also to differ. Nozzle configurations representative of several design categories currently in use, or considered for use, for aircraft propulsion systems were studied. The nozzle configurations included a (1) convergent circular nozzle, (2) bypass (2-stream) nozzle, (3) 6-tube mixer nozzle, and (4) 6-tube mixer nozzle with ejector.

Jet velocity decay characteristics for the various nozzles were obtained initially using a static test stand and then in a wind tunnel to determine forward velocity effects.

The acoustic effects of forward velocity were obtained using a free jet and a stationary microphone arena. Use of this technique can cause refraction problems due to the shear layers between the nozzle exhaust jet and free jet as well as the free jet and ambient surroundings. Refraction would tend to reduce the sound pressure level near the jet axis while increasing that near 90° to the axis. Because cold flow was used for both flow systems, the refraction effect should be minimal in the present study. Consequently, major acoustic trends between the various nozzle configurations using the present testing techniques are considered valid and representative of inflight noise characteristics.

In the subsequent sections of this report, the effect of forward velocity on jet velocity decay and jet noise are discussed separately. Finally, in the CONCLUDING REMARKS section, the relation between the aerodynamic and acoustic data trends are discussed.

APPARATUS AND PROCEDURE

Facilities

Static test stand. - The static test stand used in the present work to obtain measurements of static thrust and jet velocity decay is shown schematically in figure 1(a). Pressurized air at about 520° R is supplied to a 6-inch diameter plenum by twin diametrically opposed supply lines. Flexible couplings in each of the twin supply lines isolate the supply system from a force measuring system. The plenum is free to move axially through an overhead cable suspension system. A load cell at the upstream end of the plenum is used to measure thrust. The test nozzles were attached to a flange at the downstream end of the plenum.

Airflow through the overhead main supply line was measured with a calibrated orifice. The nominal nozzle inlet total pressure was measured with a single probe near the plenum exit flange.

A traversing probe was positioned downstream from the nozzle exit plane and radial pressure-traverses were made at various axial distances from the nozzle exit plane from 1/8 to 120 inches. Pressure measurements were obtained at nominal nozzle pressure ratios of 1.15, 1.3, 1.53, 1.87, and 2.3.

The measurements from the traversing probe were transmitted to an x-y-y' plotter which yielded direct traces on graph paper of the total and static pressure distribution radially across the jet. All other pressure data were recorded from multitube water or mercury manometers.

Wind tunnel. - The effect of forward velocity on the downstream decay of jets was studied in a Lewis 6- by 9-foot subsonic wind tunnel (ref. 3) at tunnel-air velocities up to 400 feet per second. The nozzles were mounted in the tunnel test section on struts as shown in figure 1(b). The center portion of the pod served as a plenum in the nozzle airflow system.

Pressurized air at about 520° R is supplied to the model nozzle through a strut and the plenum. Airflow through the supply line was measured with a calibrated orifice. The nominal nozzle inlet total pressure was measured with a single probe near the plenum exit flange. Jet surveys at various downstream locations from the nozzle exit plane were

made with a traversing pitot-static tube. The pressures measured with the pitot-static probe were transmitted to an x-y-y' plotter which yielded direct traces on graph paper of the total and static pressure distribution across the jet and adjacent tunnel airstream. All other pressures were recorded from mercury and water manometer boards.

Acoustic test stand. - A 13-inch diameter free jet was used to simulate aircraft forward speed. (The flow system of this rig is described in ref. 4.) The various nozzles were mounted on the centerline of the free jet, with the test nozzle exhaust plane 9 to 15 inches downstream of the free jet exhaust plane as noted in figure 1(c).

The flow system for the test nozzles, proceeding downstream, consisted of a flow control valve, two perforated plates, a four-chamber-baffled muffler, a 4-inch inlet pipe and, finally, the nozzle. The muffling system removed sufficient internal noise so that it was not significant in the measured far-field noise levels. Pressurized air was supplied at a nominal temperature of about 520° R. Data were obtained at nominal jet velocities of 670 to 1085 feet per second. Velocities were determined from measured total pressure and temperature using the isentropic equation. Free jet velocities from 0 to 260 feet per second were used in the present study.

Sound data were taken with 0.5-inch condenser microphones placed on a 10-foot radius circle centered at the nozzle exit. The microphone horizontal plane and jet centerline were located $12\frac{3}{4}$ feet above ground level. The sound data were analyzed by a 1/3 octave band spectrum analyzer. The analyzer determined sound pressure level (SPL) spectra referenced to 0.0002 microbar. Overall sound pressure levels (OASPL) and sound power level (PWL) were computed from the SPL data. Herein, no corrections are made to the data for ground reflections. Most of the cancellations and reinforcements in the data occur at much lower frequencies than the peak noise and are not pertinent to the present study.

Configurations

The nozzle configurations studied consisted of four basic types commonly considered for or used with aircraft propulsion systems; namely, a convergent circular nozzle (ref. 5), a bypass nozzle, a 6-tube mixer

nozzle (ref. 3), and, finally, a 6-tube mixer nozzle with ejector.

The convergent nozzle had a 2.06-inch diameter. Sketches of the bypass nozzle and 6-tube mixer nozzle, with and without ejector are shown in figure 2, together with pertinent dimensions. The dimensions given in figure 2(a) are for the bypass nozzle used with the free jet. The bypass nozzle used for the aerodynamic tests was similar but dimensionally 45 percent larger than that shown in figure 2(a). The secondary flow for the bypass nozzle was varied by the insertion of suitable screens upstream of the bypass exhaust plane. Photographs of typical nozzle installations in the free jet are shown in figure 3.

For the present study, data for the mixer nozzle with ejector was obtained with the ejector inlet lip located at two stations, $1\frac{5}{8}$ inches downstream and 7/8 inches upstream, relative to the mixer nozzle exhaust plane. These stations correspond, respectively, to the location for maximum thrust augmentation for this ejector and a location that yields additional shielding and absorption capability for a possible acoustically lined ejector while still providing thrust augmentation. For these two stations the thrust was augmented by 16 percent for the rearward ejector location and 7 percent for the forward ejector location. (These data are a portion of a more extensive unpublished study of the axial velocity decay associated with ejector condigurations.)

AERODYNAMIC RESULTS

The overall effects of forward velocity on a jet exhaust flow field is shown in figure 4 in which lines of constant Mach number are plotted in terms of radial and axial distance measured from and along the nozzle centerline, respectively. (All symbols used in text and on figures are defined in NOMENCLATURE.) The data shown are for the 6-tube mixer nozzle at a jet Mach number of 0.98; however, the data trends are applicable to all nozzles and jet Mach numbers studied. In general, the effect of forward velocity on a jet flow field is to reduce the rate of velocity decay with axial distance measured downstream from the nozzle exhaust plane. At a given axial station, therefore, the local velocities are generally greater with forward velocity than those measured in static conditions. In the case of the mixer nozzle data shown in figure 4, the

peak axial jet Mach number with forward velocity does not occur at the nozzle centerline until 40 inches downstream of the nozzle exhaust plane compared with 25 inches for static external flow conditions.

Velocity Profiles

The effect of forward velocity on the velocity profiles, in terms of local Mach number, at several axial stations is shown in figures 5 to 8 for the nozzles studied.

Typical velocity profiles obtained with the convergent circular nozzle are shown in figure 5. At an X/D_e of 5 (near the end of the jet core), forward velocity has not significantly altered the peak axial jet velocity nor the local radial distribution of velocity until the jet-free stream boundary is reached. At an X/D_e of 13, forward velocity has caused the peak axial jet velocity to remain about 20 percent greater than that obtained statically.

The velocity profiles for the bypass nozzle are shown in figure 6 and compared with those for a convergent nozzle of equal flow area. (It should be noted that for the bypass nozzle, the reference jet velocity is that of the core.) As the bypass flow is decreased, the radial extent and peak Mach number at a given axial station also is decreased. In the limits, the velocity profiles with decreasing bypass flow should approach those associated with a nozzle equal in size to the core of the bypass nozzle while they approach those associated with an equivalent total area nozzle size when U_s/U_c approaches 1.0. The effect of forward velocity (not shown in fig. 6) on the velocity decay of the bypass nozzle was similar to that for the convergent circular nozzle.

The 6-tube mixer nozzle provides a rapid jet velocity decay with axial distance downstream of the nozzle exhaust plane compared with a convergent nozzle of equal flow area as shown by the static data in figure 7. The effect of forward velocity on delaying axial velocity decay, however, generally is greater for the mixer nozzle than for the convergent nozzle at a given axial station. At larger axial distance downstream of the nozzle exhaust plane, $X/D_{e,T}$ of 13, the velocity profiles and the effect of forward velocity on the axial velocity decay for these two nozzles begin to be more similar.

(fig. 9(a)) is illustrative of a simple jet surrounded by a region of mixed flow. The downstream decay of the peak axial velocity is a curve that approaches an X^{-1} relationship downstream of the core flow.

The 6-tube mixer nozzle, with and without an ejector, shown in figure 9(b) is representative of multi-element nozzles and illustrates a complex mixing process. Initially the peak axial-velocity decay is substantially the same as that for an individual element. However, at some distance downstream of the nozzle exit plane, the individual jets coalesce sufficiently to form a large diameter coalescing core and a very slow peak-velocity decay occurs. Once the coalesced core has fully formed, normal mixing again occurs with an associated rapid velocity decay. The decay curve of a mixer nozzle can be divided into several regions shown in figure 9(b). Equations were developed in reference 6 to predict the departure point of the coalescing core from the single-element decay curve (point ①). From the data it can be shown that the velocity ratio in the coalescing core decay region has a slope of -0.2 with respect to axial distance (region denoted by ① to ②). The value of U/U_j at point ② was then correlated in reference 6. The slope in the fully coalesced region (beyond point ②) is again a function approaching X^{-1} as a limit.

The bypass nozzle (fig. 9(c)) can be considered a special case of the convergent nozzle in that, within the limits of the nozzle geometry noted herein, the flow field grossly falls within the constraints of a convergent nozzle having a diameter equal to the core nozzle for $U_s/U_c = 0$ and a diameter equivalent to the combined area of the core and secondary nozzles for $U_s/U_c = 1$. Thus the peak axial velocity decay curve is effectively that for a convergent nozzle but shifted to the right, as shown in figure 9(c), with increasing U_s/U_c values. At a U_s/U_c value of 1, the curve is shifted by a function of $D_{e,T}/D_e$ to the right. The slope of the curve again approaches X^{-1} at large distances from the nozzle exhaust planes.

With forward velocity, the peak axial velocity at a given axial station is greater with forward velocity than for the static condition (ref. 3). An example of this effect, taken from reference 3, is shown by the data for a circular nozzle in figure 10 in which the ratio of peak velocity to the jet exhaust velocity, U/U_j, is plotted as a function of the distance

parameter $X\left(C_n D_e \sqrt{1 + M_j}\right)^{-1}$.

Empirical correlation. - In reference 3 it was shown that for a convergent circular nozzle and a 6-tube mixer nozzle, the peak axial velocity decay with and without forward velocity could be correlated by the following empirical relationships:

$$\frac{U - U_o}{U_j - U_o} \sim \left[X\left(C_n D_e \sqrt{1 + M_j}\right)^{-1}\right]^b \tag{1}$$

where

$$b \doteq 1 + \frac{1}{3}\left[\left(\frac{U_j}{U_o}\right)^2 - 1\right]^{-1} \tag{2}$$

Figures 11 and 12 are taken from reference 3 to illustrate the degree of correlation achieved using these relationships.

The correlation of peak axial velocity decay for bypass nozzles requires additional parameters to those already given. For the present coaxial bypass nozzle, the right side of equation (1) requires an additional multiplication factor and is then given by:

$$\left\{X\left(C_n D_e \sqrt{1 + M_j}\right)^{-1}\left[1 + \left(\frac{U_s}{U_c}\right)^{1/4}\left(\frac{D_{e,T}}{D_e} - 1\right)\right]^{-1}\right\}^b \tag{3}$$

The first term in this added factor accounts for the secondary-to-core velocity ratio while the second term takes into account the total-to-core flow area ratio. Correlation of the peak axial velocity decay for the present bypass nozzle is shown in figure 13. It should be noted that the correlation does not include a term accounting for the separation distance between the core exhaust and secondary exhaust planes. Such a term was not required for the present bypass nozzle configuration. It is apparent, however, that for large separation distance inclusion of such

a term must be considered. Furthermore, the exponent 0.25 in equation (3) was shown to be 1.0 for the slot core nozzle with annular secondary flow in reference 3. Thus, it appears that this exponent is a function of core nozzle geometry. The definition of this exponent in terms of a geometry parameter is beyond the scope of the present work.

Correlation of the peak axial velocity decay for the mixer nozzle with the ejector in the rearward location was also obtained using the preceding equations as shown in figure 14(a) for M_o values of 0 and 0.26. Shown in figure 14(b) are the data for the mixer nozzle with the ejector in the forward location. In general, these data are higher than both the predicted values from the correlation equations and those with the ejector in the rearward location. The data with the ejector in the forward location appear shifted to the right on the abscissa, very much like those for the bypass nozzle before correlation. It is possible that, in the forward location of the ejector, the flow interaction of the jet flow with the ejector induced flow, U_{ej}, causes a pseudo-bypass flow effect. Correlation would then require consideration of a term U_{ej}/U_j much like the U_s/U_c term for a bypass nozzle. Such an approach, however, is beyond the scope of the present work.

In summary, the effect of forward velocity on the decay of jet exhaust flow is to stretch the jet flow field in an axial direction. Except in the jet core flow region, this causes the local peak velocity at a given downstream station, measured from the jet exhaust plane, generally to be greater with forward velocity than that with a static external flow condition. Furthermore, with forward velocity, a specific velocity in the flow field is obtained at a smaller radial distance from the nozzle (or jet) centerline than that with a static flow condition.

ACOUSTIC RESULTS

In this section, the acoustic data obtained in the present study are presented for each nozzle type. First, the free jet acoustic characteristics are presented because these establish a noise floor that limits the range of nozzle noise data. Then the nozzle acoustic data are given, beginning with measured baseline sound pressure levels for the nozzles operating without forward velocity. The effect of forward velocity on jet

noise is then shown for a given jet velocity and finally correlated by empirical relationships developed from curve-fitting the measured data. A similar development is used to present the sound power data.

Free Jet

Typical sound power spectra for the 13-inch free jet with the convergent nozzle in place but inoperative are shown by the solid curve in figure 15. The data shown are for a free jet velocity of 260 feet per second. Also shown in figure 15 are the sound power spectra with the convergent nozzle operative at nominal jet velocities of 925 and 825 feet per second and with a forward velocity of 260 feet per second. Below a frequency of about 400 Hz, the free jet is acoustically dominant. At frequencies above 400 Hz sufficient separation exists between the nozzle jet noise data and that of the free jet to yield valid nozzle jet noise measurements. With decreasing nozzle jet velocities, the acoustic separation became less. A reduction in the free jet for velocity below 260 feet per second resulted in a decrease in the free jet sound power level. Similar trends were observed for sound pressure level measurements. In general, only jet exhaust noise data separated from the free jet noise level by at least 10 dB and above 400 Hz are included in this study.

Sound Pressure Level

Baseline spectra. - Typical baseline sound pressure level spectra for the various nozzles operating statically (zero forward velocity) are presented in figures 16 to 19 as a function of the Strouhal number based on the jet velocity and the equivalent diameter based on the total nozzle exhaust area. The sound pressure levels at several jet exhaust velocities are normalized to those measured at a nominal 925 feet per second, $U_{j(ref)}$, by scaling on the 8-power velocity law. The directivity angles for which data are shown in figures 16 to 19 are 160° which is at or near the peak noise lobe and 90°. The data indicate reasonable data correlation for the convergent circular, bypass and 6-tube mixer nozzles. The increase in noise at a Strouhal number near 0.8 for the bypass nozzle (fig. 17), particularly evident at the lowest jet exhaust velocity, is prob-

ably caused by the leading edge of the wall separating the core and secondary flow passages or the struts that attach the core nozzle to the outer bypass nozzle. Decreasing the U_s/U_c ratio from 0.7 to 0.5 lowered the SPL from 2 to 3 dB at the same core velocity. In addition a greater separation of SPL values at a directivity angle of 160^o occurred with decreasing core jet velocities. The peak noise frequency (for U_s/U_c, 0.5) at this angle also was shifted to higher values by about two 1/3-octave band center frequencies with decreasing core jet velocities.

The data for the nozzles with ejectors indicate a large amount of scatter and increase in the sound pressure levels in the Strouhal number range of 0.05 to 1.0 at a directivity angle of 90^o (fig. 19(b) and (d)). Because the mixer nozzle-only shows no such scatter in sound pressure level (fig. 18), this noise is attributed to the ejector presence. Four additional noise sources to those normally associated with a nozzle can be attributed to the use of ejectors: (1) the noise caused by support struts at the inlet to the ejector, (2) ejector inlet lip noise caused by entrainment air flow, (3) flow impingement (scrubbing) of the entrained and jet flow along the ejector inside walls, and (4) edge noise caused by the shearing action of the ejector air flow at the trailing edge of the ejector. Because of the relative magnitudes of the flow velocities involved, the latter two appear the most likely causes of the increase in noise when the ejector is used compared with nozzle-only noise. Ejector inlet location relative to the nozzle exhaust plane did not appreciably affect the sound pressure spectra at 90^o. At 160^o, however, the rearward ejector location showed a suppression in sound pressure level at high frequencies compared with the nozzle only data. At this directivity angle, the forward ejector location indicated an increase in noise level at the lower frequencies and little suppression at high frequencies.

It should be noted that, for all nozzles tested, the sound pressure spectra at other directivity angles (40^o to 140^o) are similar to those shown for the 90^o angle. The absolute magnitude of the sound pressure levels, of course, is a function of the particular directivity angle.

Effect of forward velocity. - Typical variations of sound pressure level spectra with forward velocity are shown in figures 20 to 23 as a function of 1/3-octave center band frequency for all the nozzle configu-

rations tested. These data are again shown at directivity angles of 90^{o} and the peak noise lobe angle (or 160^{o}). The nominal jet exhaust velocity is 925 feet per second for all nozzle configurations.

In general, the sound pressure levels (SPL) for the nozzles are lowered from static values with increasing forward velocity. At a directivity angle of 90^{o}, the SPL attenuations due to forward velocity for the convergent, bypass and mixer nozzles are substantially broadband. The "bottoming out" of the SPL values at high frequencies for the bypass nozzle is believed to be caused by noise emanating from the core body support struts. At the peak lobe angle, however, the SPL values are not only reduced with increasing forward velocity, but also the peak SPL occurs at decreasing values of frequency with increasing forward velocities. Thus the attenuation of SPL is substantially more at high frequencies than at low frequencies.

For the ejector-nozzle configurations, similar trends in SPL reductions with forward velocity to those for the convergent and mixer nozzles are noted at a directivity angle of 160^{o}. At the 90^{o} directivity angle, however, the reductions in SPL with forward velocity for the ejector-nozzle configurations are much less than those for the other nozzle configurations. In fact with the rearward ejector location, the sound pressure spectra at the middle and high frequencies are independent of forward velocity effects (fig. 23(b)).

Overall Sound Pressure Level

The effect of forward velocity on the overall sound pressure level (OASPL) as a function of directivity angle is shown in figure 24 for all the configurations tested. The directivity angles are measured from the inlet. The data shown are for a nominal jet velocity of 925 feet per second and the trends are typical of the other jet velocities covered herein.

It is evident from the data of figure 24 that the attenuation in OASPL with forward velocity is essentially independent of directivity angle from 40^{o} to 120^{o} for all configurations. The reduction in OASPL at given forward and jet velocities is greatest for all nozzles with ejectors. The 6-tube mixer nozzle with the ejector in the rearward location showed the

least noise attenuation. The convergent circular and bypass nozzles showed a uniform OASPL attenuation with forward velocity at all angles. The data of figure 24 indicate that with a mixer-type nozzle, with and without an ejector, the peak noise lobe is shifted to somewhat lower directivity angles with increasing forward velocity and that large noise attenuation can occur in the region from the shifted peak noise lobe to the nozzle jet axis. In addition, the ejector tended to provide a more uniform radiation pattern for the OASPL as a function of directivity compared with the mixer nozzle-only pattern.

Sound Power Level

Baseline spectra. - Normalized baseline sound power level spectra at zero forward velocity are shown in figure 25 for the nozzle configurations tested. As in the case of the SPL data, the sound power level spectra (PWL's) are normalized to that obtained with a nominal jet velocity of 925 feet per second, using the 8-power velocity law, and presented in terms of the conventional Strouhal number. Using this procedure, the PWL's for the several jet velocities are reduced to substantially a single curve for each configuration. The normalized sound power level for the bypass nozzle with a U_s/U_c ratio of 0.7 was on the average 3 dB higher than that with a U_s/U_c ratio of 0.5. For the 6-tube mixer nozzle-ejector configurations, the PWL spectra for the two ejector locations were substantially the same; consequently, only that for the forward ejector location is shown in figure 25. The sound power levels for the nozzles with the ejectors compared with that for the mixer-nozzle only (solid curve in fig. 25(e)) were increased by nearly 5 dB at the low frequencies, but slightly reduced at the high frequencies. (Possible causes for this increase were discussed in the previous section concerned with sound pressure spectra.) The slight deviation of the highest velocity data (triangle symbols, fig. 25(e)) from those at the lower velocities at high frequencies is due to a small amount of shock noise (jet pressure ratio of 2.1) that begins to appear as a noise source.

Effect of forward velocity. - Typical variations of sound power spectra with forward velocity for the various nozzle configurations are shown in figure 26. All data are shown for a nominal jet velocity of

925 feet per second. The sound power level, in general, is reduced on a broadband basis with increasing forward velocity for all configurations; however, the amount of PWL attenuation is dependent on the particular nozzle configuration. The largest sound power attenuations occurred with the convergent and mixer nozzles, while the least occurred with the mixer nozzle-ejector configuration having the ejector in the rearward location. For these latter nozzle configurations, the reduction in sound power level with increasing forward velocity is least at high frequencies.

Total sound power. - The total sound powers for the various nozzle configurations used are shown in figure 27 as a function of relative velocity, $U_j - U_o$. (U_j for the bypass nozzle is the core jet velocity.) Also shown, by the solid line, is the 8-power velocity law. The solid symbols in figure 27 represent the total sound power measurements with zero forward velocity. Good agreement of the static acoustic data with the 8-power velocity law generally is apparent. For the mixer nozzles with ejector, the total sound power at the low jet exhaust velocity is substantially higher than predicted by the 8-power velocity law. This increase is due to the additional noise noted previously in the discussion of the sound pressure spectra and attributed to the jet scrubbing on the ejector walls and ejector trailing edge noise. At the lower jet velocities this noise source becomes dominant. As a consequence, acoustic data at a jet velocity of 670 feet per second were not used in the correlation efforts discussed later herein.

With increasing forward velocity, the total sound power is increasingly attenuated; however, the attenuated total power levels do not correlate with relative velocity and, hence, do not fall on the static (jet velocity) curve. The deviation of the acoustic data with forward velocity from the static curve depends primarily on the nozzle configuration and the absolute forward velocity. It should be noted that data for the convergent circular, bypass and 6-tube mixer nozzles show substantially the same effect of forward velocity, while the two ejector-nozzle configurations showed much less effect of forward velocity at a given jet velocity. These trends are consistent with the SPL and PWL data discussed in the preceding sections.

Acoustic Data Correlation

The acoustic data presented in preceding sections show that forward velocity effects can cause significant differences in jet exhaust noise attenuation, depending on nozzle geometry and flow considerations. An effort was made to obtain preliminary acoustic correlation parameters for the nozzle configurations used in the present study. For correlation purposes, the jet exhaust noise attenuation due to forward velocity effects was determined not only from overall acoustic values (OASPL and total power), but also from consideration of the differences between the SPL and PWL spectra for each configuration. The correlation parameters were weighted more to acoustic data taken at forward velocities of 175 feet per second or less than to acoustic data taken at 260 feet per second because of possible acoustic refraction effects that would be more severe at high forward velocities than at low velocities. In addition, the introduction of noise sources, other than jet exhaust noise, at forward velocities of 260 feet per second lent more credence to acoustic data taken at 175 feet per second and less. Acoustic data taken with a jet velocity of 670 feet per second also exhibited extraneous noise floor problems for some configurations and such data were discounted for correlation purposes. It should be emphasized that the empirical correlation parameters shown in this section apply only to the nozzle geometries tested. The correlation parameters developed on the basis of the present data are summarized in table I.

In table I, the U*-velocity terms normalize the sound pressure and sound power levels, while the V*-velocity term is used to obtain, where necessary, modified Strouhal numbers. Total sound power measurements are correlated by plotting as a function of U_3^*.

By applying these correlation parameters, the acoustic data herein were correlated as shown in figures 28 to 31. In general, the sound pressure level spectra at a directivity angle of 90^o (fig. 28) correlated on the conventional Strouhal number, but the SPL reduction varied as a function of the jet velocity, U_j, and relative velocity, $U_j - U_o$, given by U_1^* in table I. At a directivity angle near the peak lobe, the correlation parameter differed markedly for each type of nozzle configuration. An

example of the correlation of the data at 160^{o} is shown in figure 29 for the convergent nozzle.

Correlation of sound power level spectra (fig. 30) showed that the same parameters correlated the convergent circular, bypass and 6-tube mixer nozzle data. The ejector-nozzle configurations, however, required parameters that differed from each other as well as from the more conventional nozzles. The total sound power variation with jet and forward velocities (fig. 31) was correlated by the same parameters that correlated the level of the sound power spectra for the various nozzles. Also, these same parameters correlate the OASPL reasonable well.

CONCLUDING REMARKS

From the results of this exploratory study, it is quite apparent that the attenuation of jet exhaust noise by forward velocity depends on the nozzle configuration. For cold air jet exhaust flows that interact directly with the surrounding environment, including convergent, bypass and multi-element mixer nozzles, the effect of forward velocity on the jet noise levels of interest can be estimated, as a first order approximation, by the use of a velocity parameter $U_j(1 - U_o/U_j)^{3/4}$. The noise attenuation appears to be caused by a reduction in shear at the jet boundary due to forward velocity. However, the attenuation mechanism is influenced by changes in the jet structure itself due to forward velocity. These changes include longer axial core lengths and altered velocity profiles in a direction normal to the jet axis.

The difference between the experimentally determined exponent of 3/4 and that of 7/8 obtained by taking the 1/8 power of the Ffowcs Williams expression given in reference 2 may be due to refraction effects attributable to the test facility. It can be argued, however, that because cold flow was used the experimental data are not significantly affected and that the 3/4-exponent is, perhaps, more likely the correct value.

For nozzles in which the jet exhaust flow does not interact directly with the surrounding environment, such as a nozzle with ejector, the effect of forward velocity on jet noise can be much less, to almost negligible, compared with that when direct interaction occurs. It appears

that if the ejector is flowing full, the forward velocity affects primarily the acoustics associated with the flow out of the ejector exhaust plane. With a nozzle, high frequency noise generally is associated with a location near the nozzle exit plane while continually lower frequency noise occurs with increasing distances downstream of the nozzle exit plane, for up to twice the jet core length. Thus, when a mixer nozzle with ejector is used, the dominant noise sources from the many small nozzles are frequently located within the length of the ejector. Consequently, when the jet flow exhausts at the ejector exit plane, the resultant low jet velocity while interacting with forward velocity, is no longer a major noise source. This is the case for present mixer nozzle with ejector in the rearward location. The major noise sources are contained within the ejector and surrounded by entrainment flow that renders these noise sources essentially independent of the external flow (forward velocity). Consequently, only small effects of forward velocity were obtained, except in the low frequency range associated with the jet downstream of the ejector exhaust plane.

The mixer nozzle with the ejector located forward, on the other hand, still shows a very high jet velocity at the ejector exhaust plane. This high velocity jet constitutes a loud noise source and, because it is located downstream of the ejector exhaust plane, is subject to significant forward velocity effects that can be beneficial from the point of view of jet noise suppression. For an actual aircraft installation using a multi-element nozzle of 30 or more elements together with an ejector, it is quite reasonable to expect little noise suppression due to forward velocity for the high frequencies associated with the multi-element jet flow inside the ejector, but reductions in noise level could be expected to occur for the lower frequencies of the augmented jet downstream of the ejector exhaust plane. Lining the ejector, as has been demonstrated frequently, will reduce the high frequency, internal mixing noise within the ejector.

NOMENCLATURE

(English units, except as noted)

C_n	effective nozzle coefficient
D_e	effective core diameter of nozzle or single element
$D_{e,T}$	effective diameter of total nozzle area
f	1/3 octave band spectrum frequency
M	local Mach number
M_j	jet exhaust Mach number
M_o	free stream Mach number
OASPL	overall sound pressure level, dB re 20 μ N/m^2
PWL	sound power level, dB re 10^{-13} W
SPL	sound pressure level, dB re 0.0002 microbar
U	local peak velocity
U_c	core exhaust velocity
U_{ej}	ejector inflow velocity
U_j	jet exhaust velocity
$U_{j(ref)}$	reference jet velocity for normalization, 925 ft/sec
U_o	free stream velocity
U_s	secondary exhaust velocity
U^*, V^*	velocity correlation parameters
X	axial distance downstream of nozzle exhaust plane

REFERENCES

1. Coles, W. D., Mihaloew, J. A., and Swann, W. H., "Ground and In-Flight Acoustic and Performance Characteristics of Jet-Aircraft Exhaust Noise Suppressors," TN D-874, 1961, NASA, Cleveland, Ohio.

2. Ffowcs Williams, J. E., "The Noise From Turbulence Convected at High Speed," Philosophical Transactions of the Royal Society of London, Ser. A, Vol. 255, No. 1061, Apr. 18, 1963, pp. 469-503.

3. von Glahn, U., Sekas, N., Groesbeck, D., and Huff, R., "Forward Flight Effects on Mixer Nozzle Design and Noise Considerations for STOL Externally Blown Flap Systems," TM X-68102, 1972, NASA, Cleveland, Ohio.

4. Dorsch, R. G., and Reshotko, M., "EBF Noise Tests with Engine Under and Over the Wing Configuration," STOL Technology, SP-320, NASA, Washington, D.C.

5. Olsen, W. A., Dorsch, R. G., and Miles, J. H., "Noise Produced by a Small-Scale Externally Blown Flap," TN D-6636, 1972, NASA, Cleveland, Ohio.

6. von Glahn, U. H., Groesbeck, D. E., and Huff, R. G., "Peak Axial-Velocity Decay With Single- and Multi-Element Nozzles," Paper 72-48, Jan. 1972, AIAA, New York, N.Y.

TABLE I. - ACOUSTIC CORRELATION PARAMETERS

Nozzle	SPL at 90°	SPL at 160°		PWL
	U_1^*	U_2^*	V^*	U_3^*
Convergent	$U_j\left(1 - \frac{U_o}{U_j}\right)^{3/4}$	$U_j\left(1 - \frac{U_o}{U_j}\right)^{3/4}$	$(U_j - U_o)$	$U_j\left(1 - \frac{U_o}{U_j}\right)^{3/4}$
Bypass	$U_j\left(1 - \frac{U_o}{U_j}\right)^{3/4}$	$U_j\left(1 - \frac{U_o}{U_j}\right)^{3/4}$	U_j	$U_j\left(1 - \frac{U_o}{U_j}\right)^{3/4}$
Mixer	$U_j\left(1 - \frac{U_o}{U_j}\right)^{3/4}$	$U_j\left(1 - \frac{U_o}{U_j}\right)^{7/8}$	$\frac{(U_j - U_o)^3}{(U_j)^2}$	$U_j\left(1 - \frac{U_o}{U_j}\right)^{3/4}$
Mixer + forward ejector	$U_j\left(1 - \frac{U_o}{U_j}\right)^{1/4}$	$U_j - U_o$	$\frac{(U_j - U_o)^3}{(U_j)^2}$	$U_j\left(1 - \frac{U_o}{U_j}\right)^{1/2}$
Mixer + rearward ejector	U_j	$U_j\left(1 - \frac{U_o}{U_j}\right)^{1/2}$	$(U_j - U_o)$	$U_j\left(1 - \frac{U_o}{U_j}\right)^{1/4}$

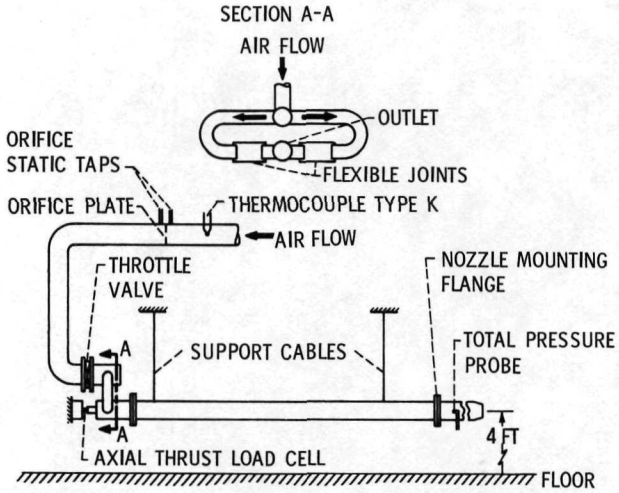

(a) SCHEMATIC DIAGRAM OF TEST RIG FOR STATIC AERODYNAMIC MEASUREMENTS.

Figure 1. - Test rig details.

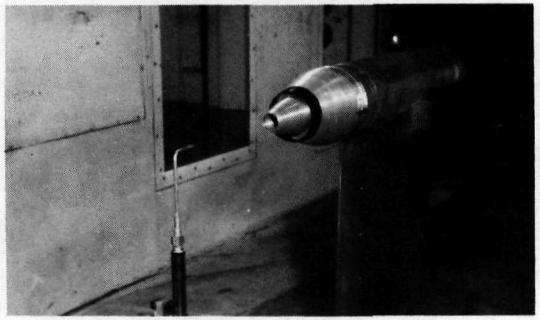

(b) BYPASS NOZZLE INSTALLED IN 6x9-FOOT WIND TUNNEL FOR AERODYNAMIC MEASUREMENTS WITH FORWARD VELOCITY.

	DIMENSIONS, IN.	
	E	y
CONVERGENT CIRCULAR	9.0	4
BYPASS	13.25	4
6-TUBE MIXER (WITH AND WITHOUT EJECTOR)	15.0	6

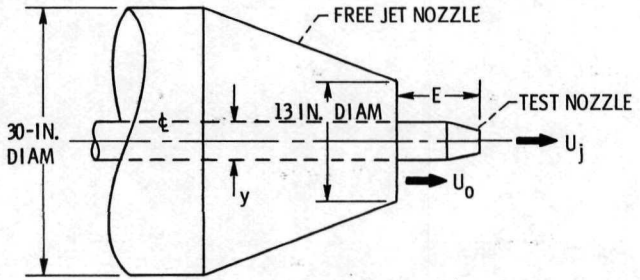

(c) TEST NOZZLE INSTALLATION IN FREE JET FOR ACOUSTIC MEASUREMENTS.

Figure 1. - Concluded.

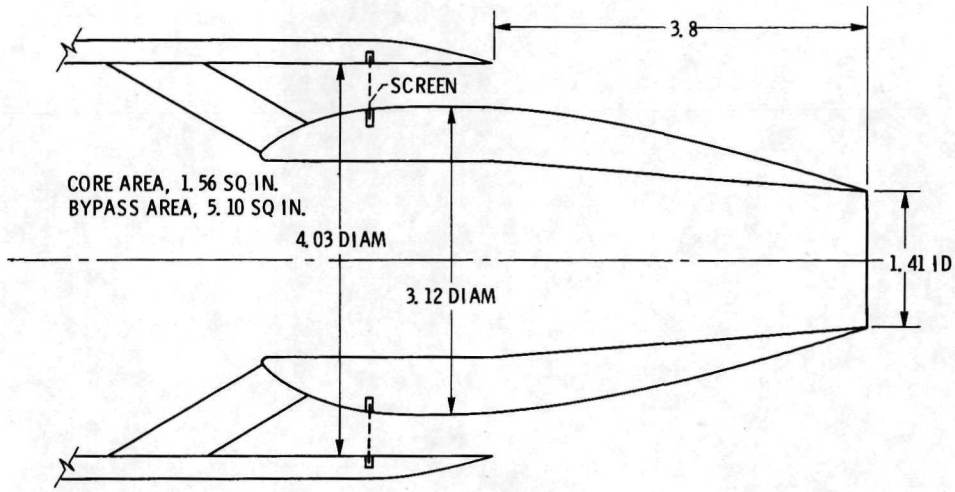

(a) BYPASS NOZZLE.

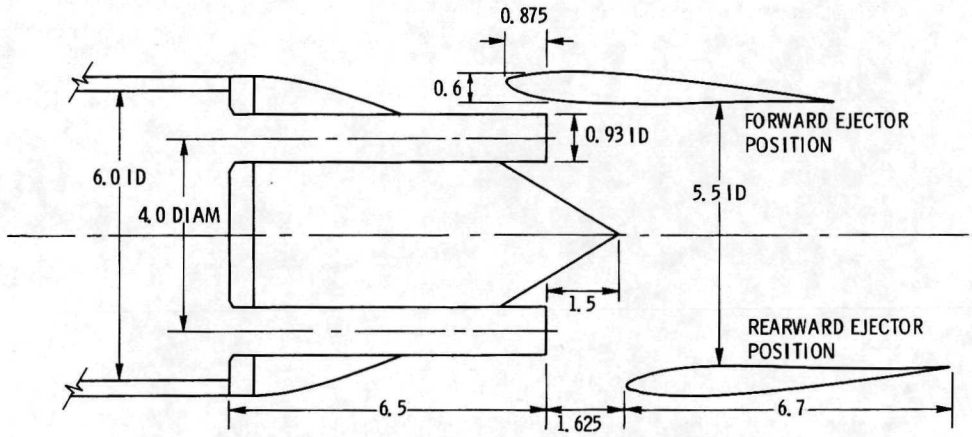

(b) 6-TUBE MIXER NOZZLE WITH AND WITHOUT EJECTOR.

Figure 2. - Nozzle dimensions. (All dimensions are in in.)

(a) 6-TUBE MIXER NOZZLE.

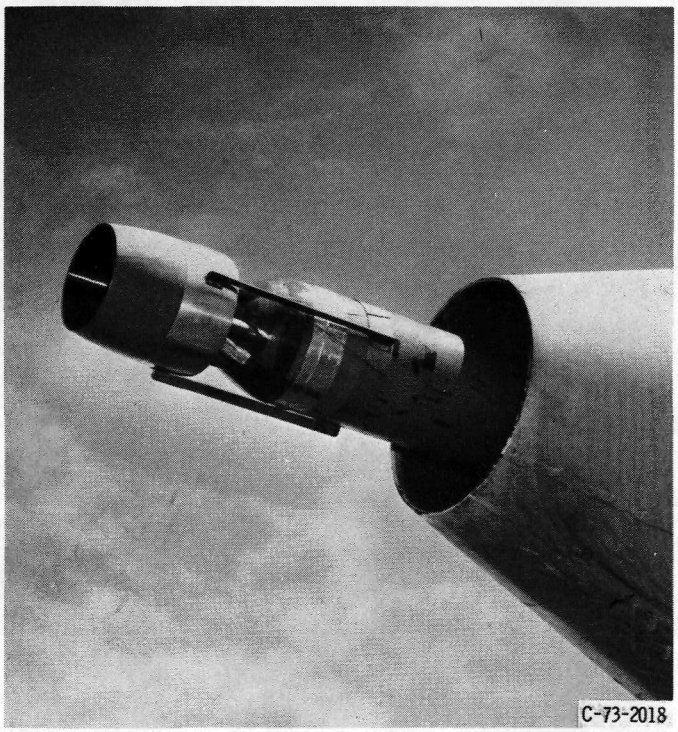

(b) 6-TUBE MIXER NOZZLE WITH EJECTOR.

Figure 3. - Photographs showing typical nozzles mounted on free jet.

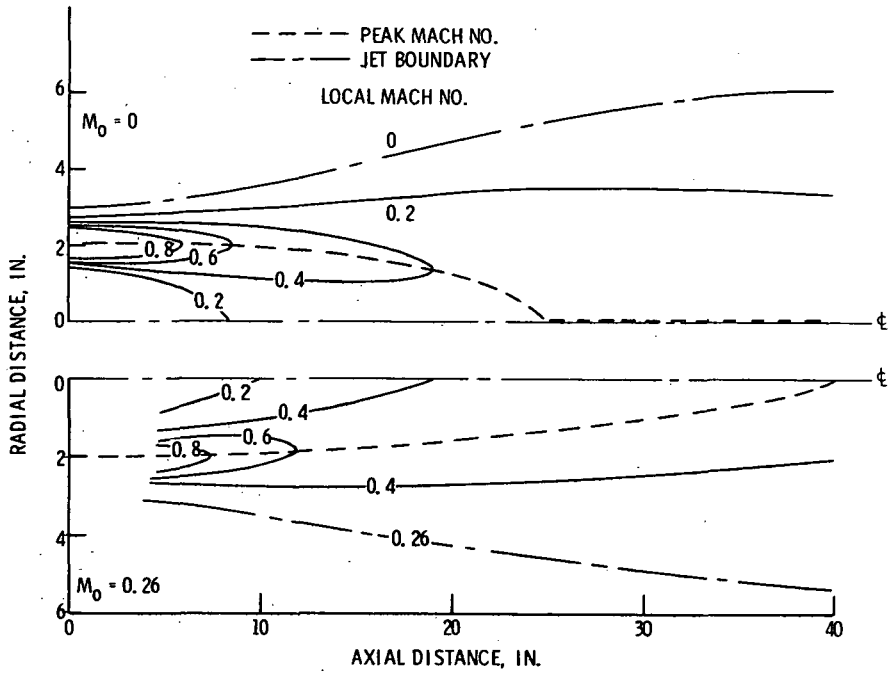

Figure 4. - Comparison of typical jet flow fields with and without forward velocity. 6-Tube mixer nozzle; jet Mach number, 0.98.

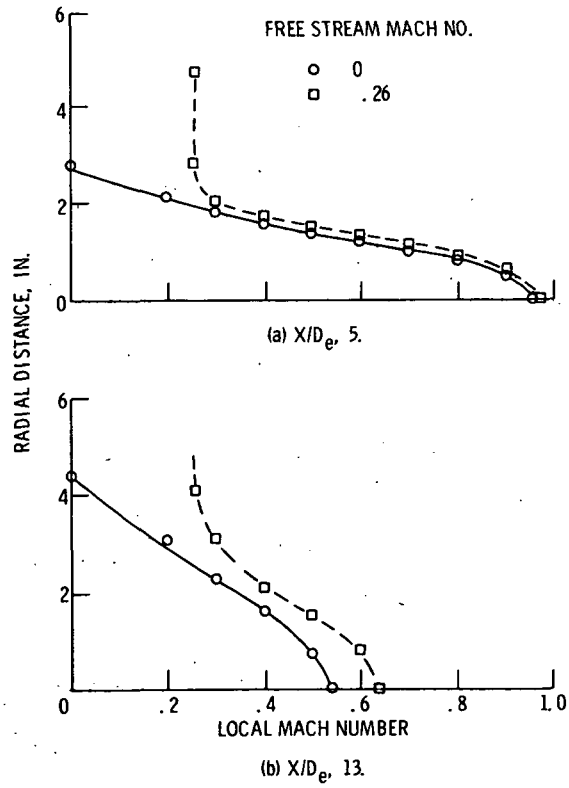

(a) X/D_e, 5.

(b) X/D_e, 13.

Figure 5. - Velocity profiles for convergent circular nozzle with and without forward velocity. Jet Mach number, 0.98.

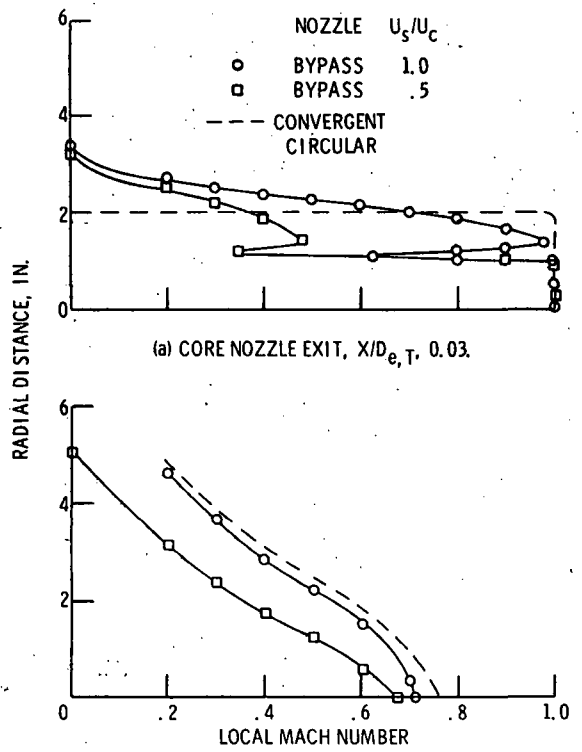

(a) CORE NOZZLE EXIT, $X/D_{e,T}$, 0.03.

(b) $X/D_{e,T}$, 9.0.

Figure 6. - Typical velocity profiles for bypass nozzle. Zero forward velocity; core jet Mach number, 0.98.

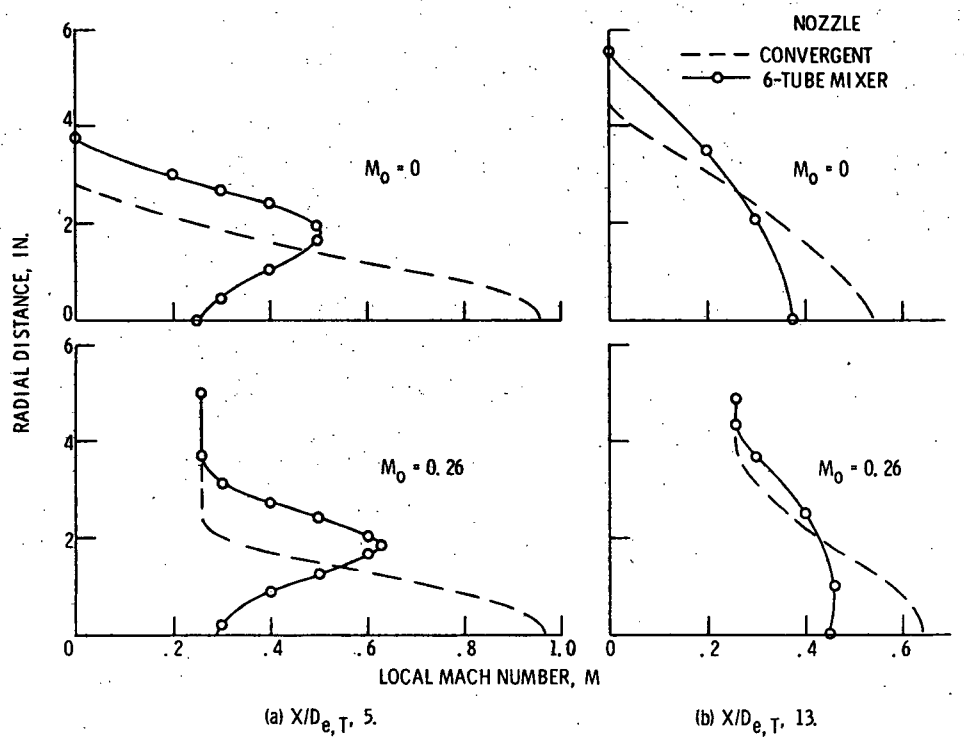

(a) $X/D_{e,T}$, 5.

(b) $X/D_{e,T}$, 13.

Figure 7. - Velocity profiles of 6-tube mixer nozzle with and without forward velocity. Jet Mach number, 0.98.

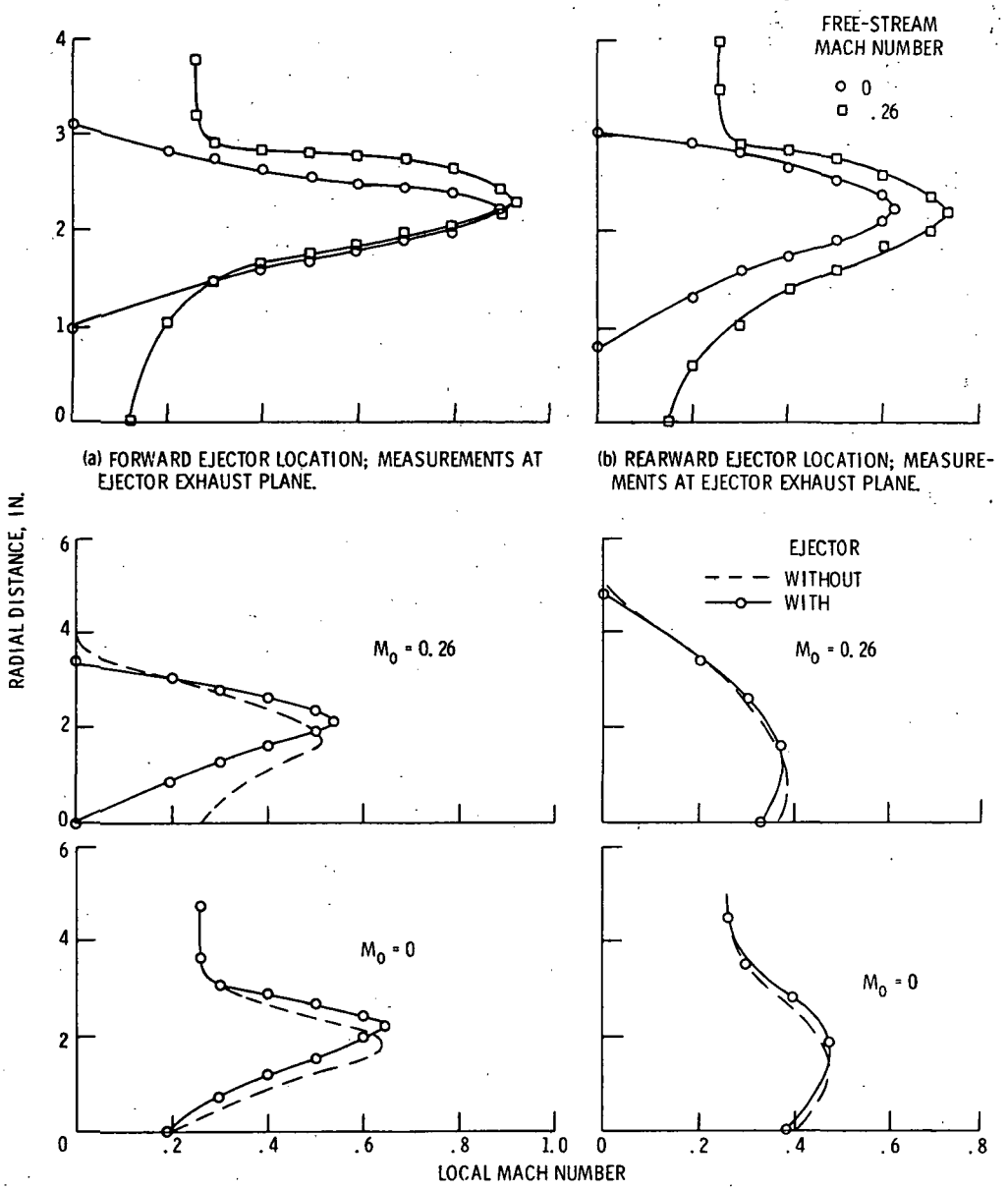

Figure 8. - Effect of ejector on velocity profiles for 6-tube mixer nozzle, with and without forward velocity. Jet Mach number, 0.98.

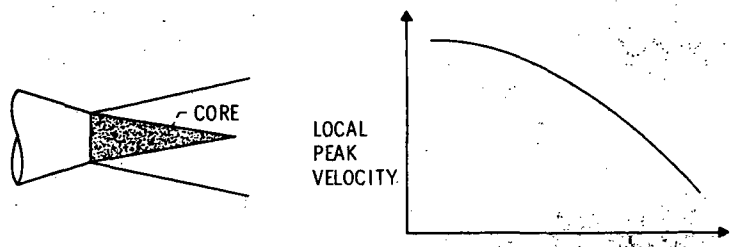

(a) CONVERGENT CIRCULAR NOZZLE.

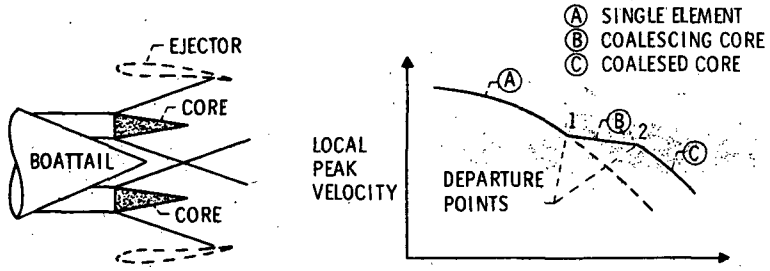

(b) 6-TUBE MIXER NOZZLE; WITH AND WITHOUT EJECTOR.

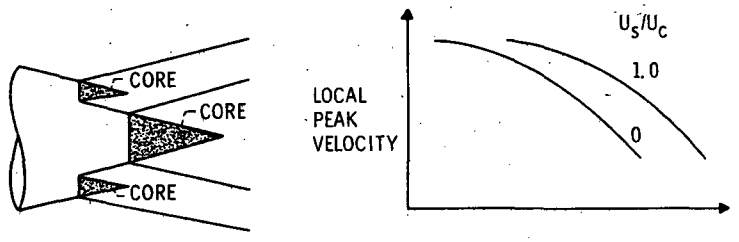

(c) BYPASS NOZZLE.

Figure 9. - Schematic flow-mixing patterns and typical peak axial velocity decay for various nozzle configurations. Zero forward velocity.

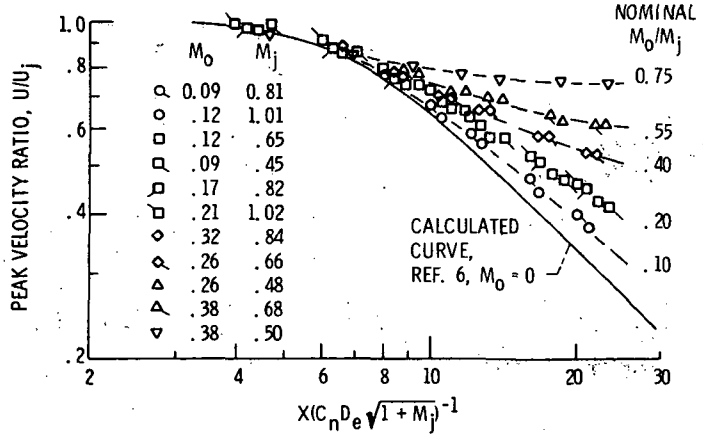

Figure 10. - Velocity decay for convergent nozzle with forward velocity. C_n, 0.77; reference 3.

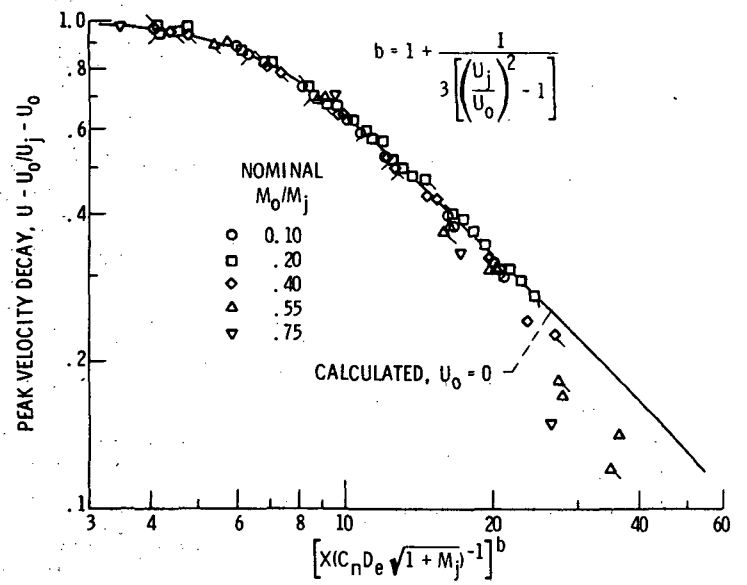

Figure 11. - Correlation of relative velocity decay for convergent circular nozzle. C_n, 0.77; reference 3.

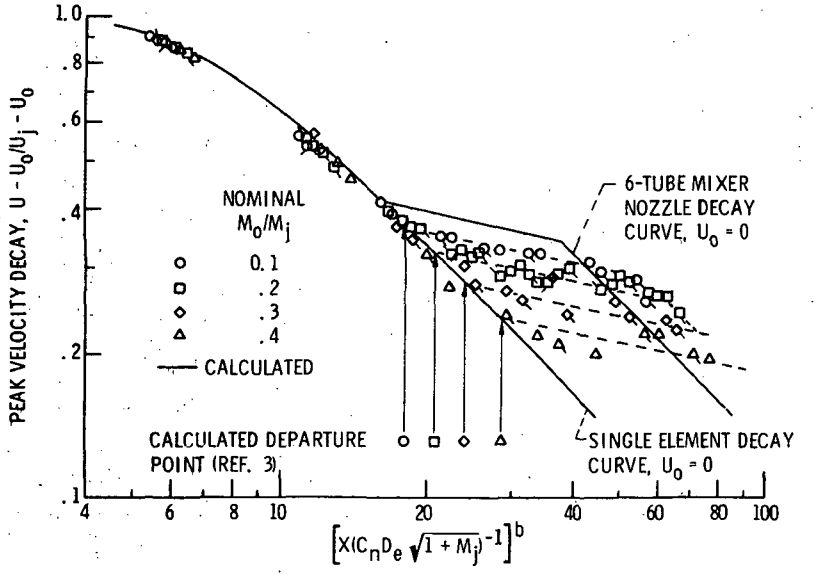

Figure 12. - Correlation of relative velocity decay for mixer nozzle. C_n, 0.7; reference 3.

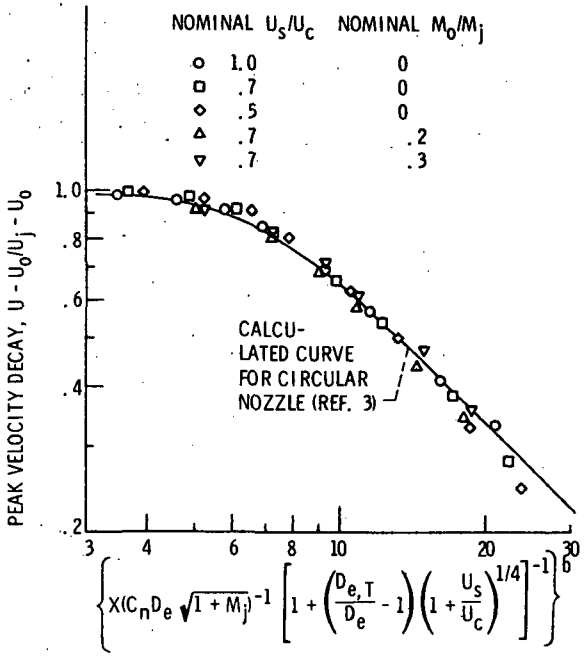

Figure 13. - Correlated relative velocity decay for bypass nozzle. Core jet Mach number, 0.98; C_n, 0.75.

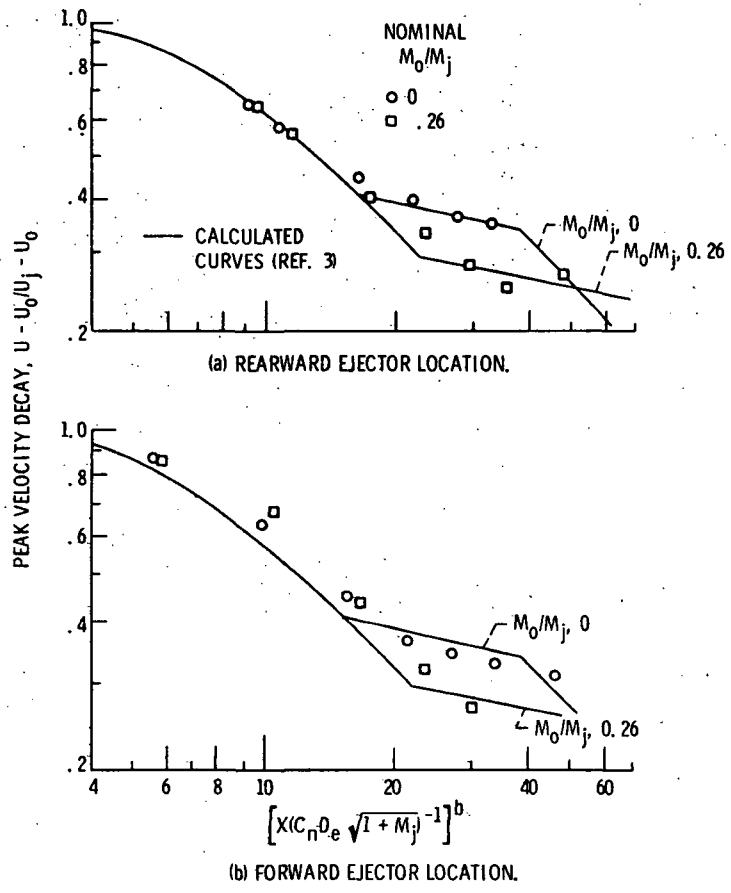

Figure 14. - Correlated relative velocity decay for 6-tube mixer nozzle with ejector. Jet Mach number, 0.98.

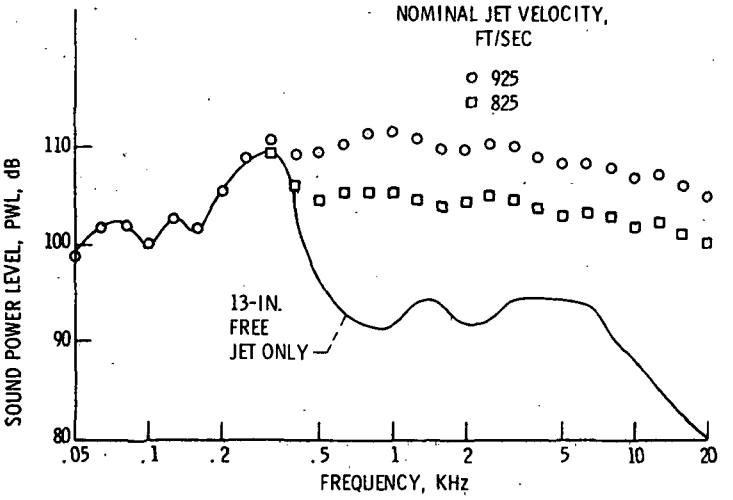

Figure 15. - Comparison of sound power level spectra for free jet with and without operation of a test nozzle. Free jet velocity, 260 ft/sec.

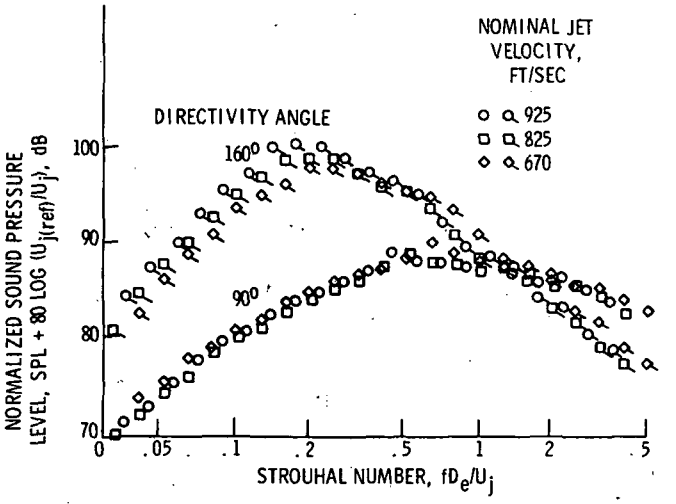

Figure 16. - Normalized sound pressure level spectra for convergent circular nozzle at zero forward velocity.

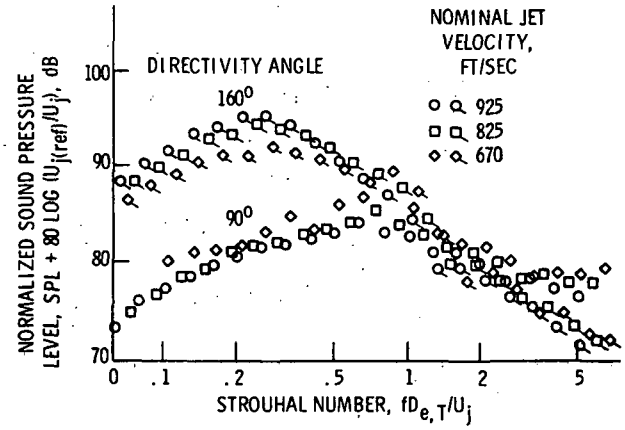

Figure 17. - Normalized sound pressure level spectra for bypass nozzle at zero forward velocity. Nominal U_s/U_c, 0.7.

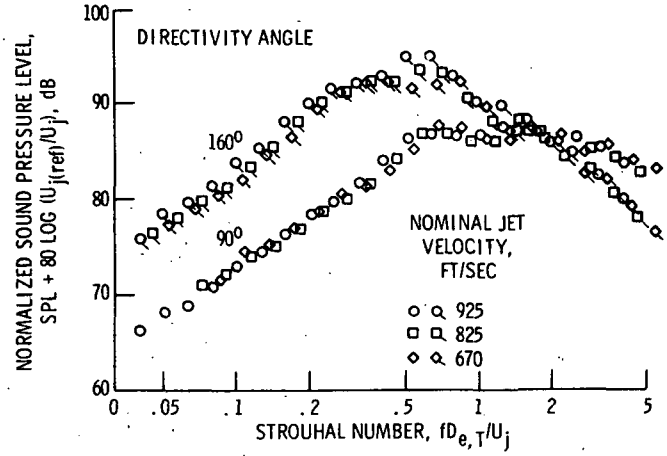

Figure 18. - Normalized sound pressure level spectra for 6-tube mixer nozzle at zero forward velocity.

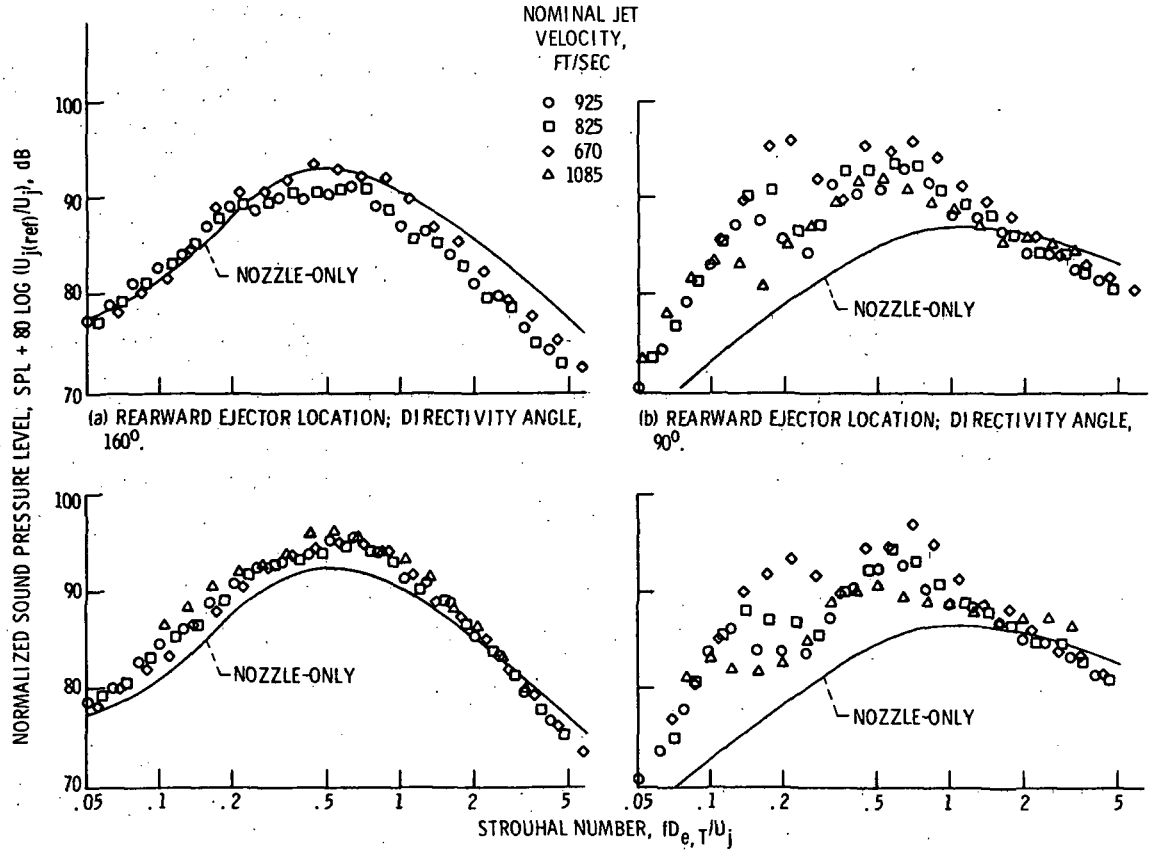

(a) REARWARD EJECTOR LOCATION; DIRECTIVITY ANGLE, 160°.

(b) REARWARD EJECTOR LOCATION; DIRECTIVITY ANGLE, 90°.

(c) FORWARD EJECTOR LOCATION; DIRECTIVITY ANGLE, 160°.

(d) FORWARD EJECTOR LOCATION; DIRECTIVITY ANGLE, 90°.

Figure 19. - Normalized sound pressure level spectra for 6-tube mixer nozzle with ejector. Zero forward velocity.

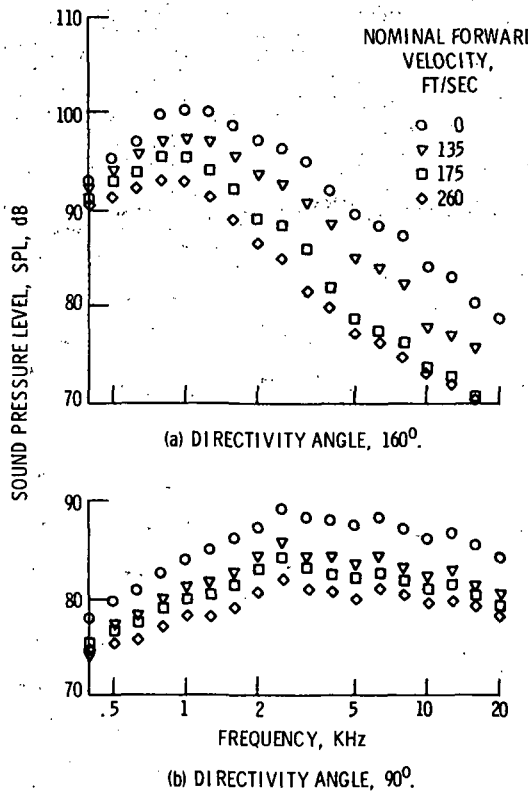

Figure 20. - Effect of forward velocity on sound pressure level spectra for a convergent circular nozzle. Nominal jet velocity, 925 ft/sec.

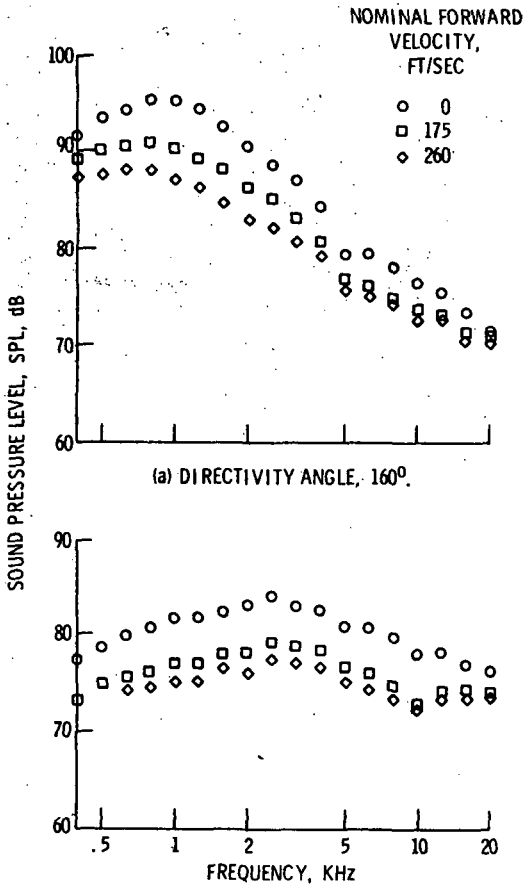

Figure 21. - Effect of forward velocity on sound pressure level spectra for a bypass nozzle. Nominal U_s/U_c, 0.7; nominal core jet velocity, 925 ft/sec.

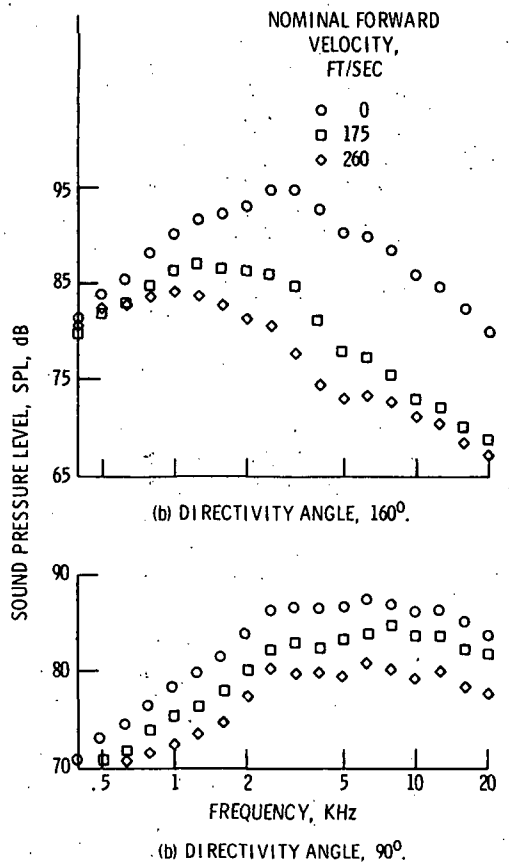

Figure 22. - Effect of forward velocity on sound pressure level spectra for a 6-tube mixer nozzle. Nominal jet velocity, 925 ft/sec.

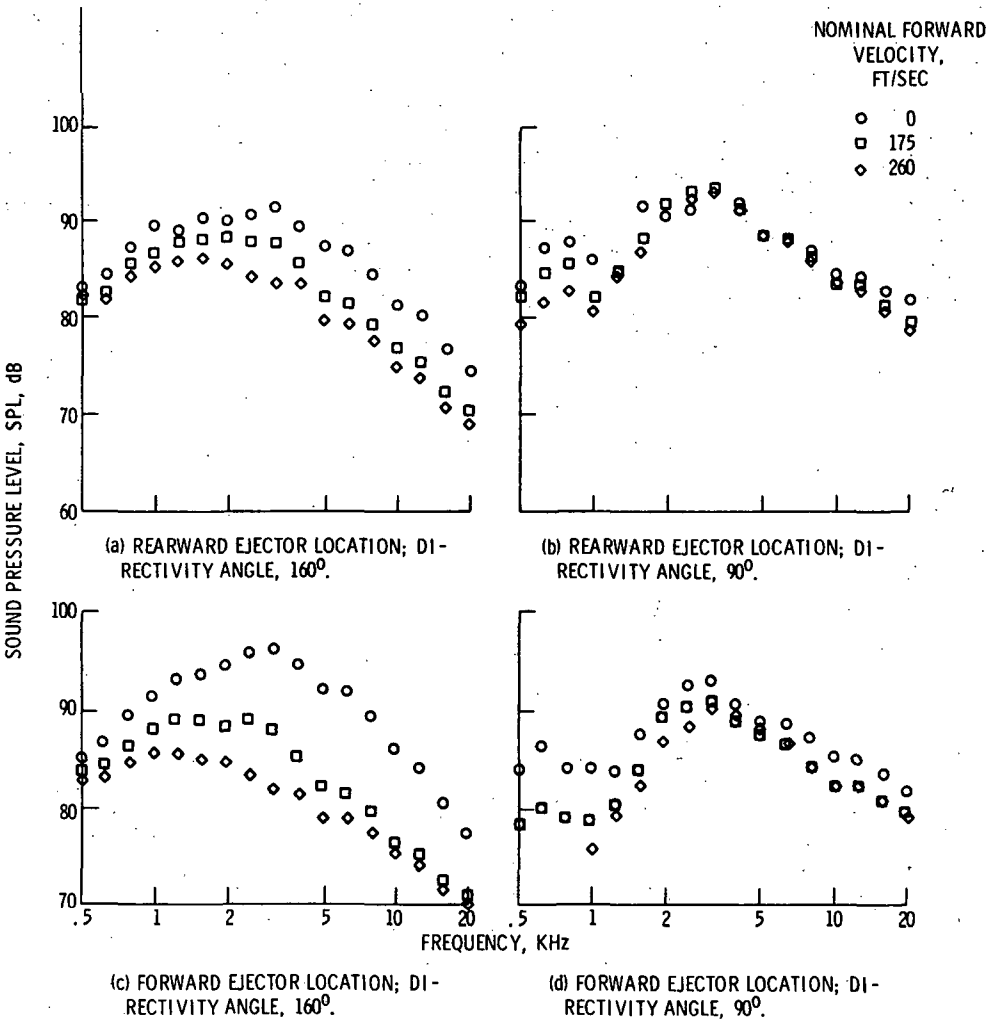

Figure 23. - Effect of forward velocity on sound pressure level spectra for 6-tube mixer nozzle with ejector. Nominal jet velocity, 925 ft/sec.

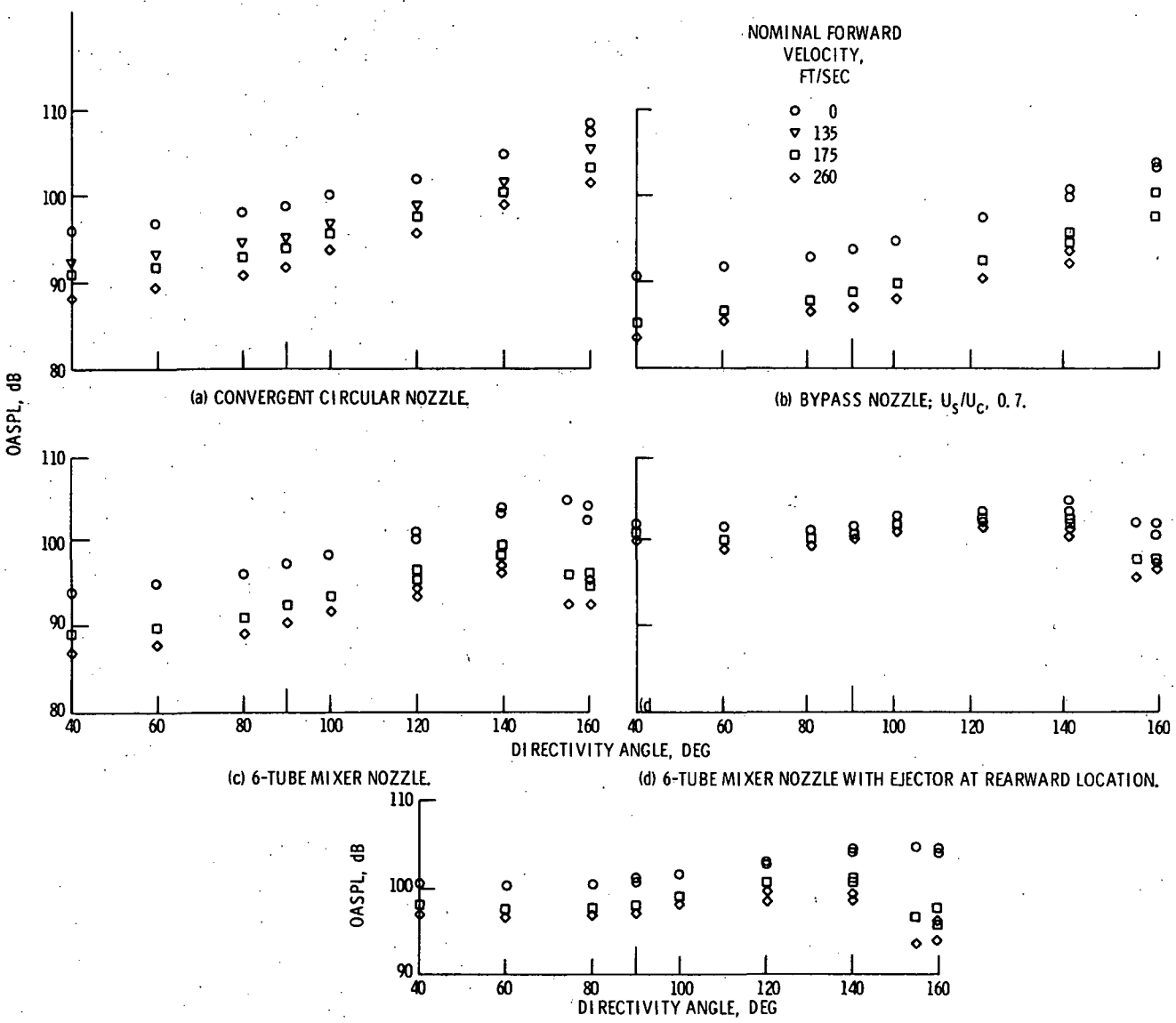

Figure 24. - Variation of OASPL with directivity angle. Nominal jet velocity, 925 ft/sec.

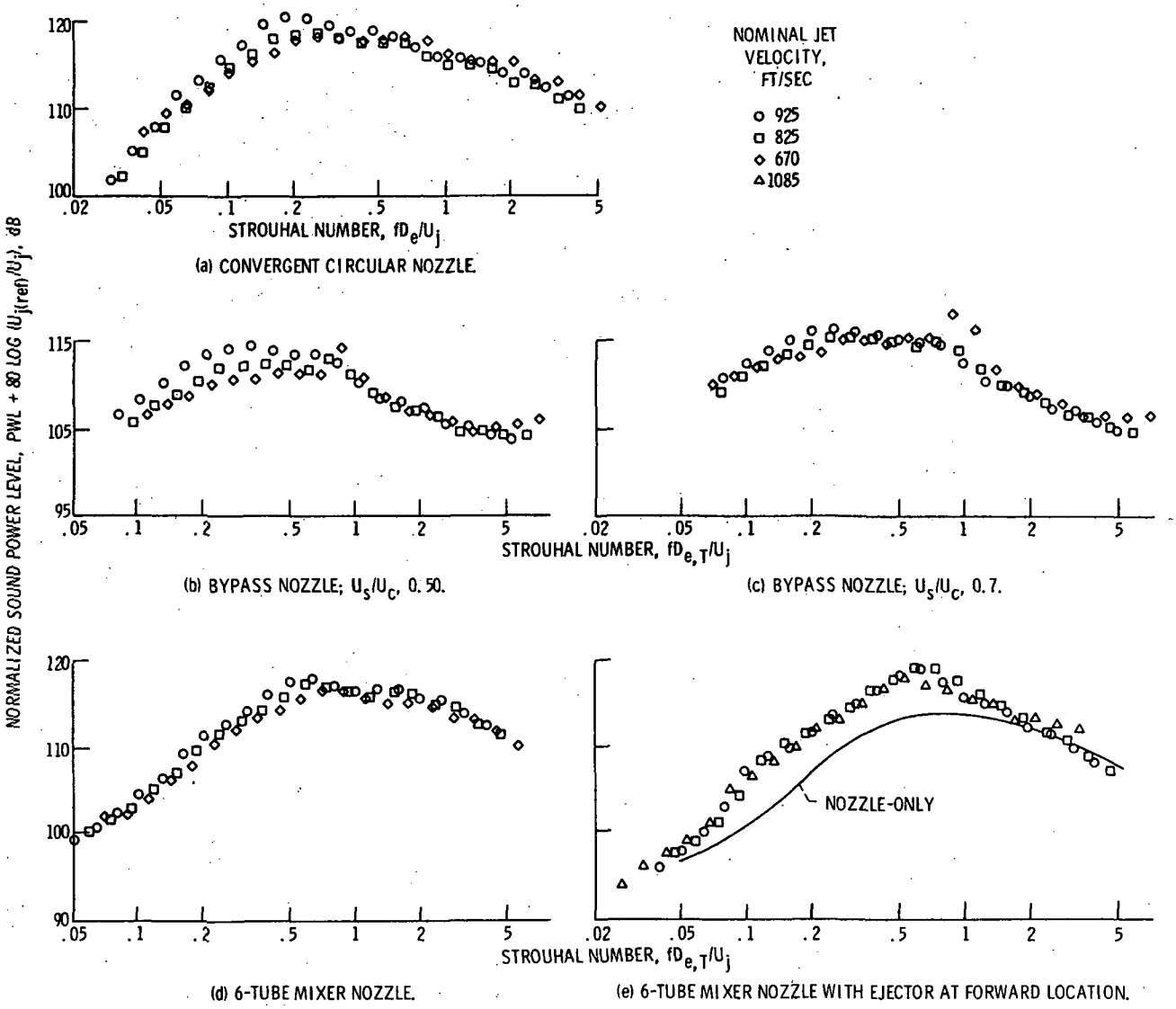

(a) CONVERGENT CIRCULAR NOZZLE.

(b) BYPASS NOZZLE; U_s/U_c, 0.50.

(c) BYPASS NOZZLE; U_s/U_c, 0.7.

(d) 6-TUBE MIXER NOZZLE.

(e) 6-TUBE MIXER NOZZLE WITH EJECTOR AT FORWARD LOCATION.

Figure 25. - Normalized sound power level spectra for nozzles tested. Zero forward velocity.

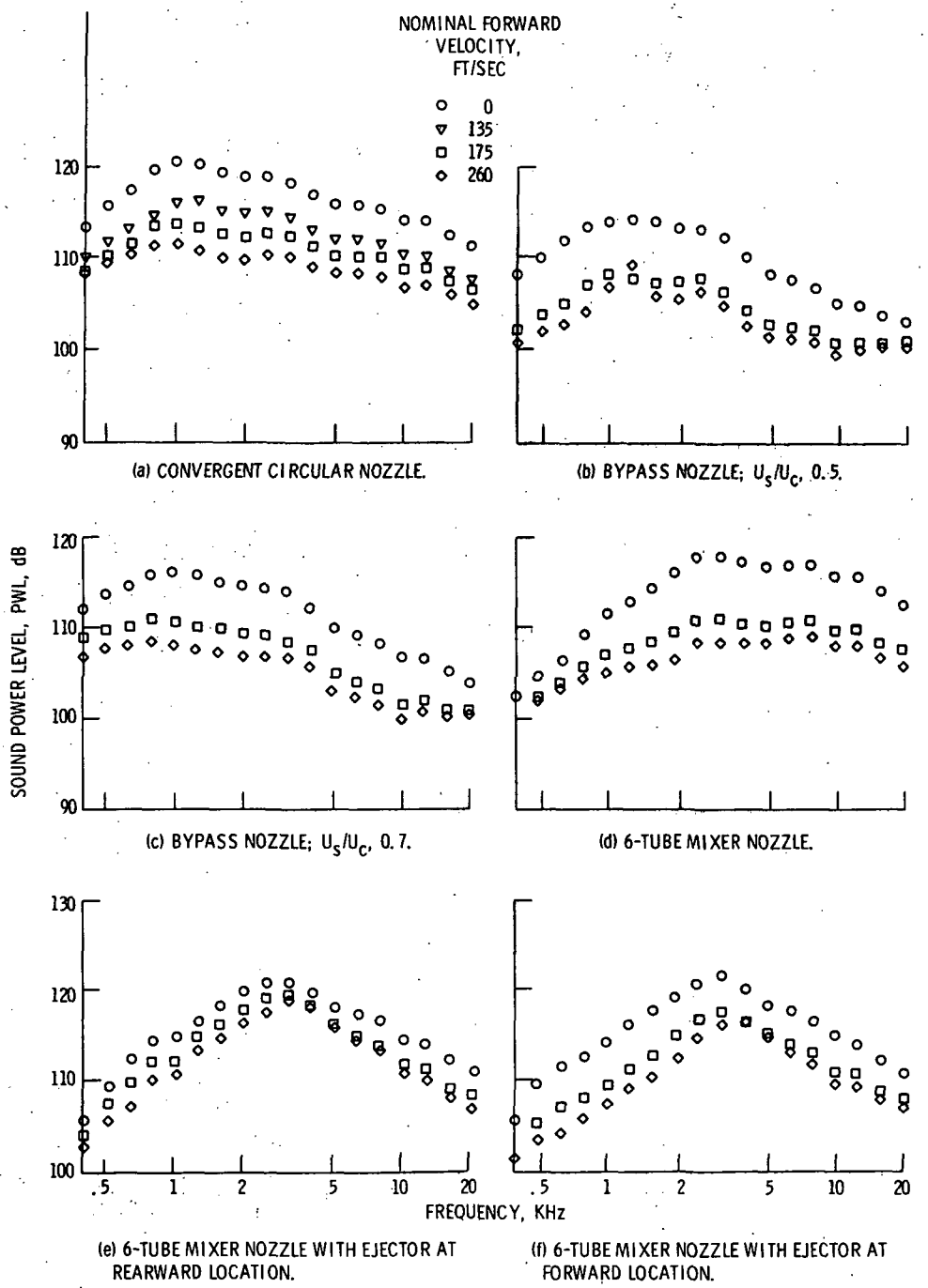

Figure 26. - Effect of forward velocity on sound power level spectra. Nominal jet velocity, 925 ft/sec.

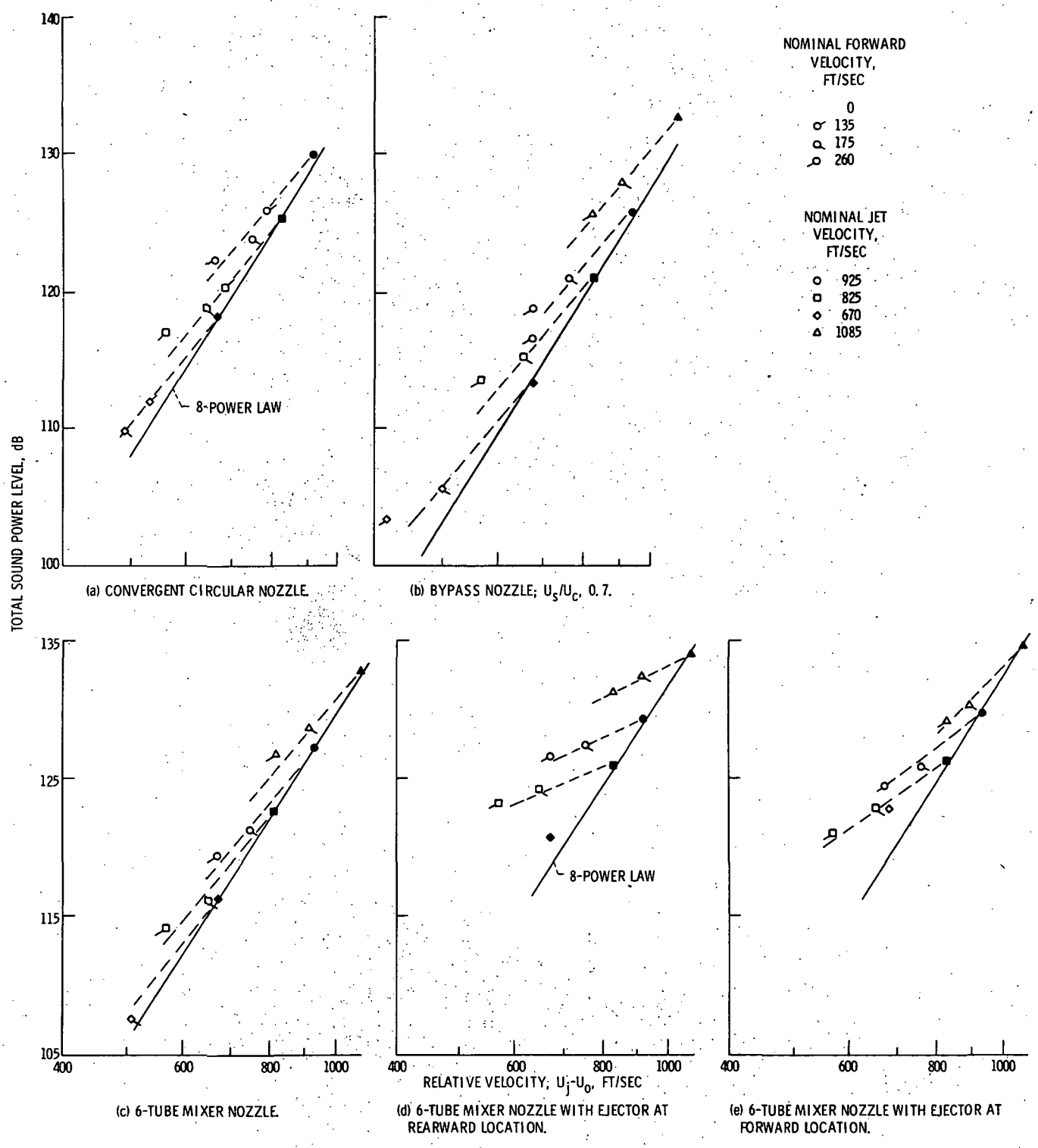

Figure 27. - Total sound power level variation with relative velocity, U_j-U_0.

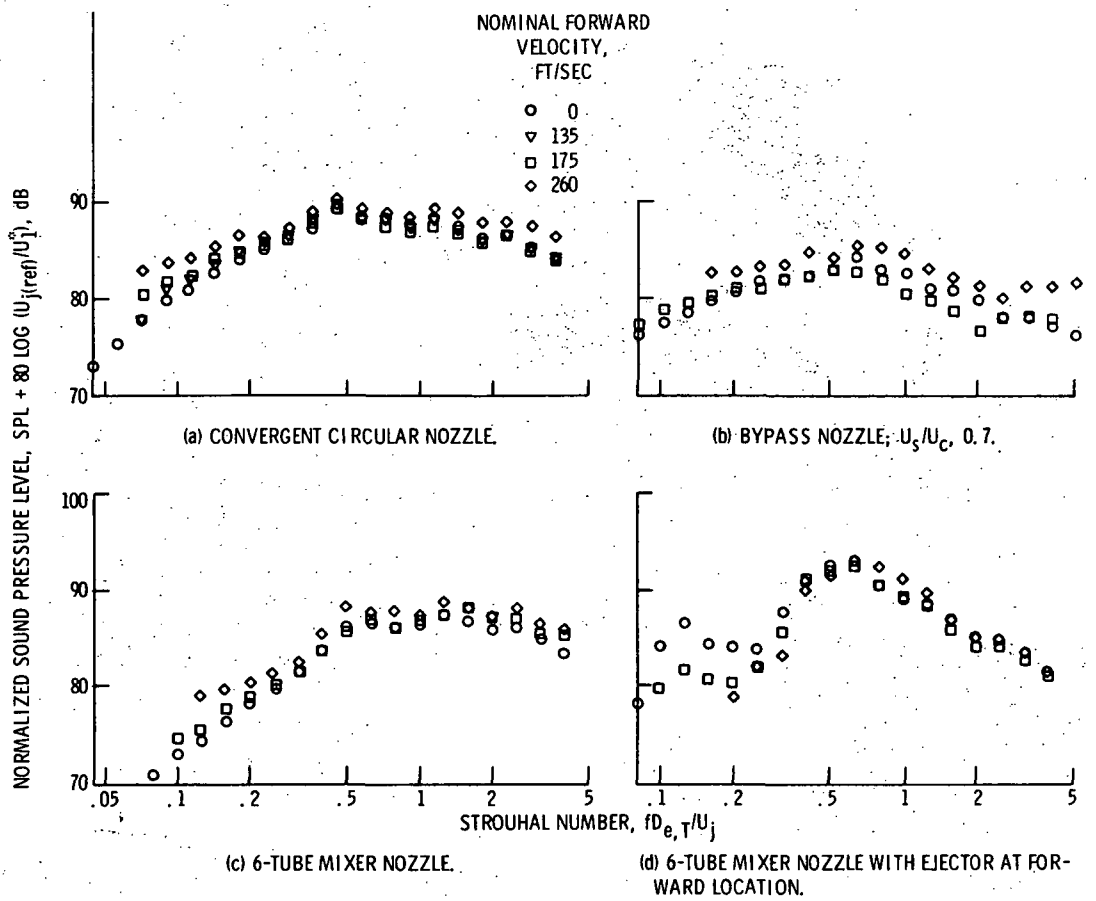

Figure 28. - Correlation of sound pressure level spectra with forward velocity. Directivity angle, 90°.

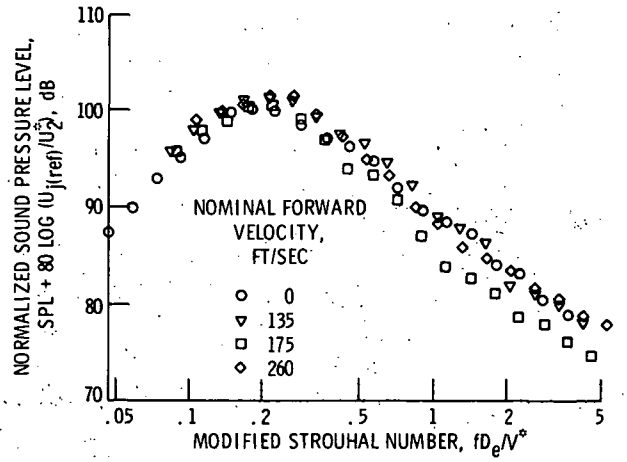

Figure 29. - Correlation of sound pressure level spectra with forward velocity. Convergent nozzle; directivity angle, 160°.

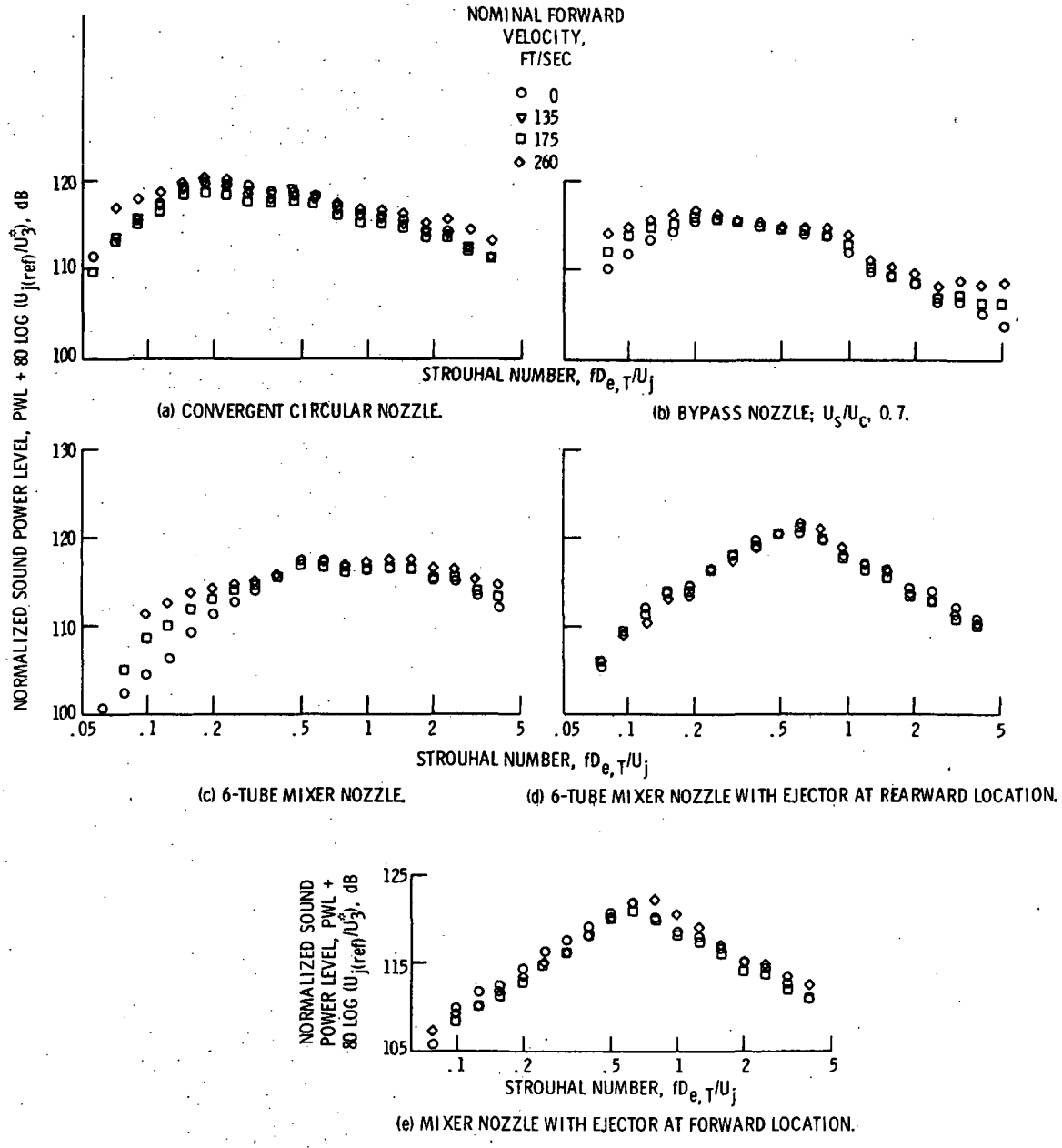

Figure 30. - Correlation of sound power spectra with forward velocity.

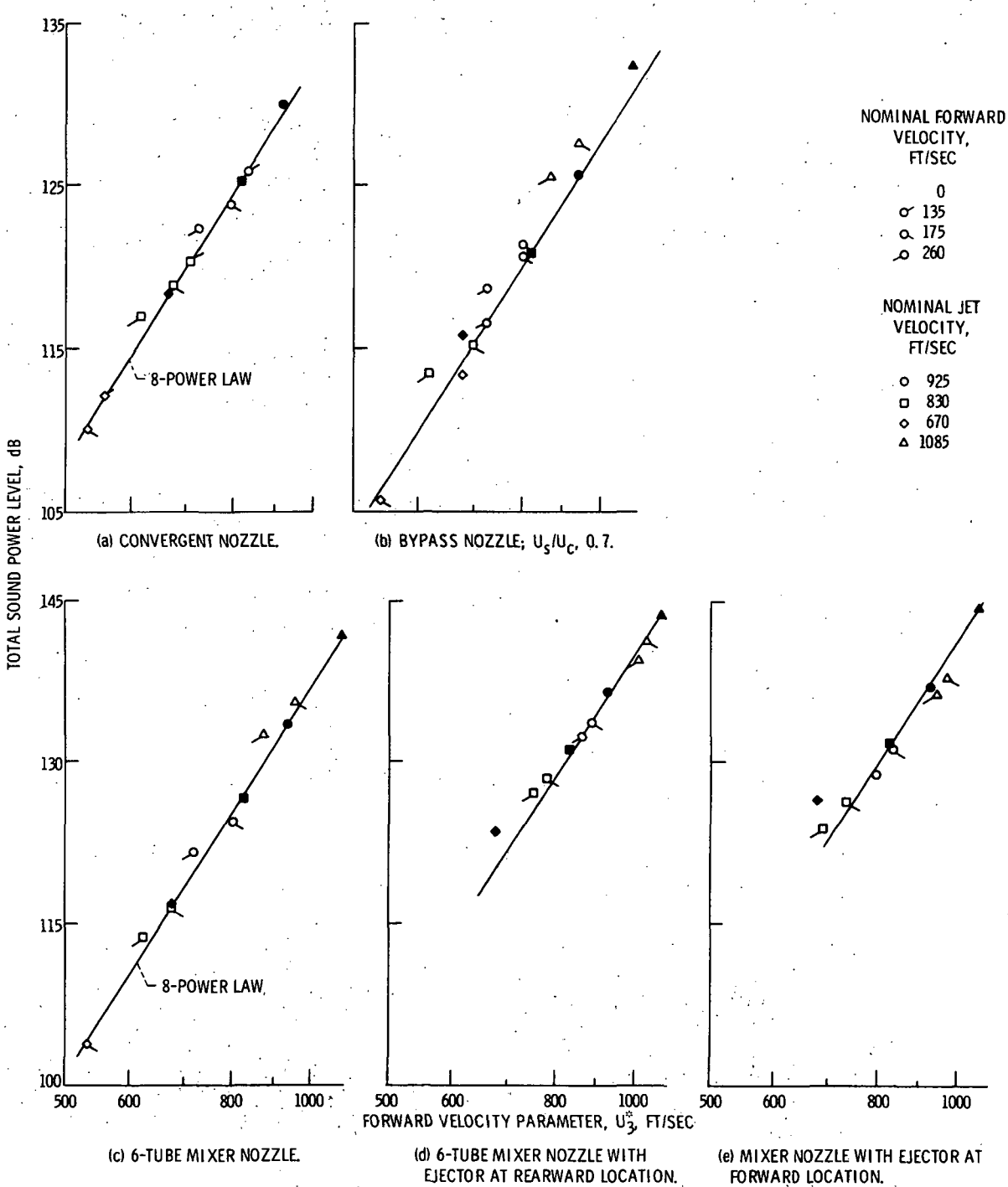

Figure 31. - Correlation of total sound power level with forward velocity.

E-7547

NASA-Lewis